STUDY OF MICROSTRUCTURE, HARDNESS AND AGING BEHAVIOUR OF 2014 ALUMINUM ALLOY

[1]SURESH CHAND, [2]MADHUSUDHAN D, [3]K. B. SRAVANI, [4]A. UMA, [5]V. SINDHU, [6]S. PADMINI DEVI, [7]G. PADMAVA

[1,2]Lecturer, [3,7]Student, Dept. of Metallurgical and Materials Engineering, RGUKT IIIT Nuzvid, A. P, India
E-mail: [1]saropya@gmail.com, [2]madhudasari@gmail.com

Abstract- The mechanical properties of aluminum alloy are purely dependent on the rate at which the alloy is heated and quenched. The commercially available aluminum alloys has potential applications in the field of aircraft. The effect aging behavior of aerospace aluminum AA2014 alloy on microstructure, hardness and XRD patterns has been studied. In order to achieve good mechanical properties of Al−Cu alloys, precipitation hardening and artificial aging treatment were applied. Solution treatment has been carried out at 542˚C for 3:30 hrs followed by quenching in water. Then artificial aging is carried out at 183 ˚C for 2 to12 hrs. The results show that after aging of 8 hours AA2014 aluminum alloy acquires maximum hardness (129.2 BHN). By the XRD analysis, we found the major peaks at 39.13˚, 45.53˚, 65.83˚, 78.8˚ and 83.17^o respectively in as received specimen. In solution heat treated sample, the peaks are found at 38.82˚, 45.14˚, 65.5˚and 78.5˚ respectively. These peaks are identified as single phase (α- Al). In artificially aged 2014 aluminum alloy for 8 hours , peaks are found at 38.59˚, 44.91˚, 65.30˚and 78.48˚ respectively. Here, only single peak of $CuAl_2$ is detected at 78.48˚on (004) plane.

Keywords- Aluminum alloy, Aging, Hardness, Heat treatment, X-ray Diffraction.

I. INTRODUCTION

The tensile strength of the 2011 alloy increases with increasing the solution temperatures, after reaching to a maximum value of 342 MPa at 525 °C, it starts decreasing with further increase in temperature. The elongation increases upto 525 °C and then decreases with increasing the solution temperature [1]. Etching of specimen with Tucker reagent for 10 second results that precipitates of Al_2Cu were etched out and grain boundaries were clearly visible [2]. Aluminum alloys are strengthen by heat treatment method subject to alloy should have such alloy element which can form coherent preicipitate. Aluminum 2014 alloy responds heat treatment. It contains copper, manganese, magnesium and silicon as principle alloying elements. This alloy is important for aerospace and army vehicle applications [3,4]. The requirement of aluminum alloy in the form of sheets with high strength has increased [5]. The strength of alloy is improved by grain refinement and precipitation hardening techniques significantly. The Equal Channel Angular Pressing, Cryorolling, Accumulating Roll Bonding, Friction Stir Processing and High Pressure Torsion techniques are used to process the aluminum alloys to develop outstanding properties [6]. Out of these processes the cryorolling is most effective method to manufacture sheets of ultrafine or nanostructured grains [7]. This process involves effective suppression of dynamic recovery due to metal working at cryogenic temperature. This treatment leads to increase in dislocation density [8-10]. The grain size less than 100 nm is termed as nanocrytalline materials. If the grain size is in range of 100-1000 nm then it is called ultra fine grain material [11]. Ultra fine structure exhibit better impact toughness at high and low strain rates [12]. Less investigation has been made to study age hardenable alloys compared to non heat treatable aluminum alloys [13-16]. Some investigations have been made on thermal stability of Al-Cu alloys consisting ultra fine structure [19-22]. The possible precipitates in 2014 alloys are $CuAl_2$, $Al_5Cu_2Mg_8Si_5$ and Mg_2Si [17-18]. The kinetics of grain growth of various ultrafine structures has been studies prepared by cryomillig, equal channel angular pressing and accumulative roll bonding [23-25].

II. DETAILS EXPERIMENTAL

The aluminum alloy AA2014 was received as extruded square rod of cross section 20 mm x 20 mm. The Six samples of the dimensions 15 mm x 10 mm x 10 mm were separated from as received sample. For microstructural observations, the sample surfaces were prepared carefully by polishing. The specimens were polished using emery papers of grits 200, 400, 600, 800 and 1000. The fine polishing was performed by using a suspension of 1µm alumina powders in distilled water on a cloth fixed to a rotating wheel. The alumina power is outstanding to remove the twin layer of metal. The samples were carefully washed to remove all abrasive after fine polishing. Samples are etched to reveal the grain structure using Keller's reagent (2.5ml Nitric acid (HNO_3)**,** 1.5 ml Hydrochloric acid (HCl)**,** 1.0 ml Hydrogen fluoride (HF) and 95 ml Distilled water). After etching samples were cleaned in running water and dried. The microstructures were analyzed under the metallurgical optical microscope at various magnifications. The samples were solution treated at 542 ^{o} C in a muffle type heat treatment furnace for 3 hours and 30 minutes. The samples were then quenched into water to get the supersaturated solid solution of α-Al. The artificial aging was carried out for six solutionized samples. The samples were subjected to age hardening at 183 ^{o} C for duration of 2, 4, 6, 8, 10 and 12 hours. The hardness was measured on Brinell Hardness Testing Machine with 10 mm ball indentor and 500 kgf loads. The samples were scanned in the X-ray diffraction machine and the scanning rate was chosen 0.5 degree per minute in the range of angle 20˚-80˚. The data is plotted in origin and analyzed.

Table 1: Chemical composition of AA2014 alloy.

Element	Cu	Mn	Si	Mg	Al
Wt %	5.28	0.4	0.45	0.2	balance

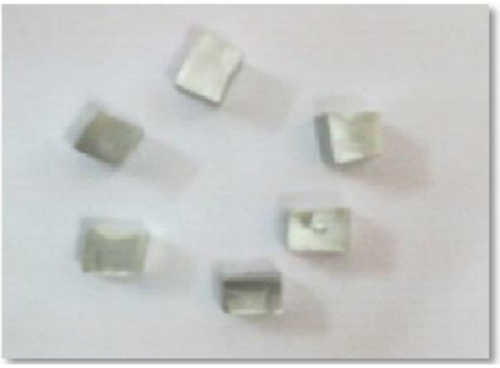

Fig.1. Image of AA2014 alloy sample.

III. RESULTS AND DISCUSSION

3.1 MICROSTRUCTURAL ANALYSIS

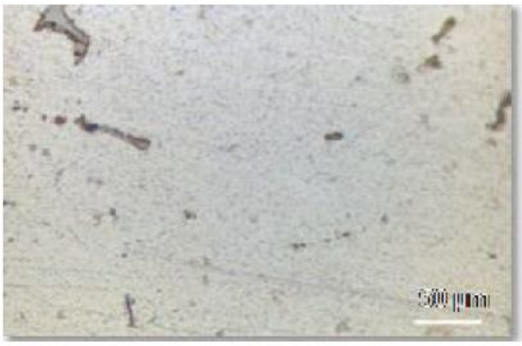

Fig.2. Optical microstructure of artificially aged 2014 aluminum alloy at 183 ^{o}C, 4 hrs.

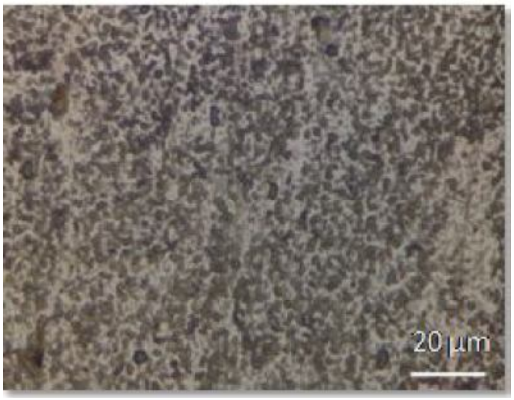

Fig.3. Optical microstructure of artificially aged 2014 aluminum alloy at 183 ^{o}C, 6 hrs.

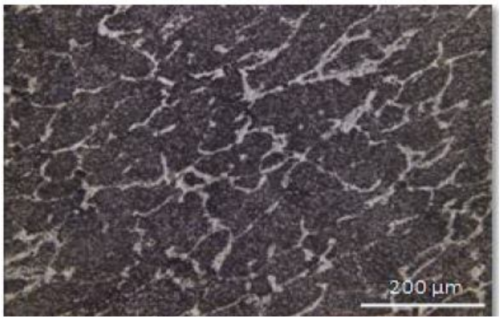

Fig.4. Optical microstructure of artificially aged 2014 aluminum alloy at 183 ^{o}C, 8 hrs.

The microstructure shown above represents maximum number of $CuAl_2$ particle. These precipitate particles are coherent with matrix.

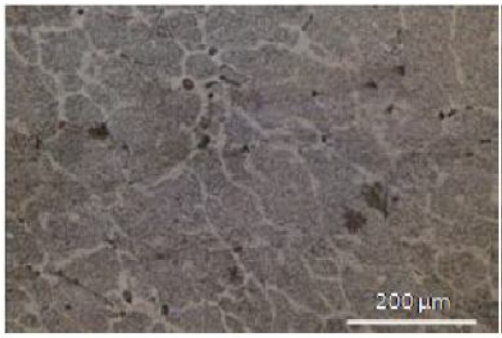

Fig.5. Optical microstructure of artificially aged 2014 aluminum alloy at 183 ^{o}C, 12 hrs.

3.2 X-RAY DIFFRACTION ANALYSIS

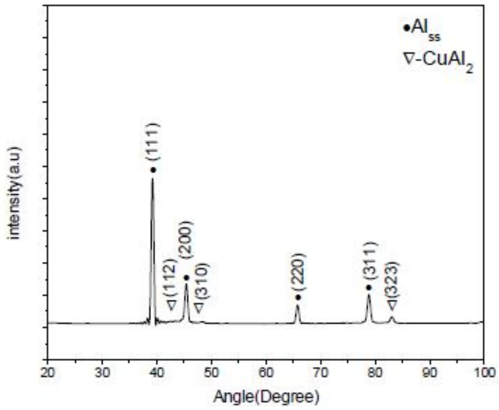

Fig.6. The XRD pattern of as received AA 2014 aluminum alloy.

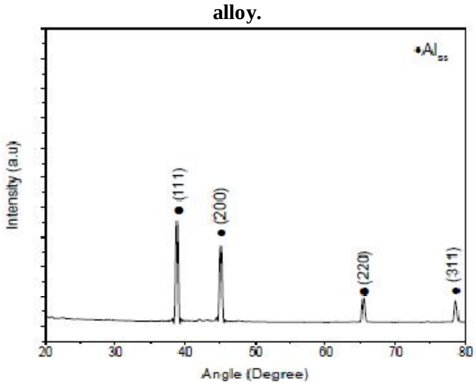

Fig.7. The XRD pattern of solution treated 2014 aluminum alloy at 542 ˚C, 3:30 hrs.

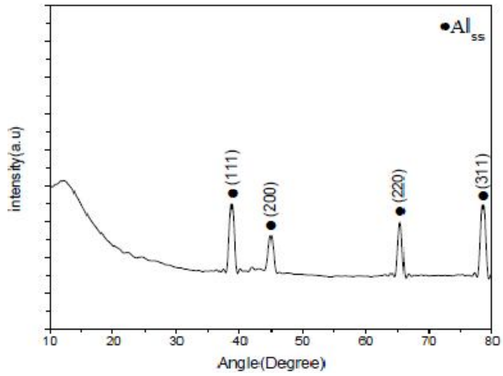

Fig.8. The XRD pattern of artificially aged 2014 aluminum alloy at 183 ˚C, 2 hrs.

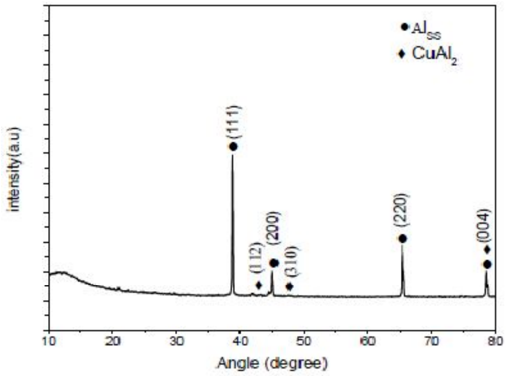

Fig.9 The XRD pattern of artificially aged 2014 aluminum alloy at 183 ˚C, 4 hrs.

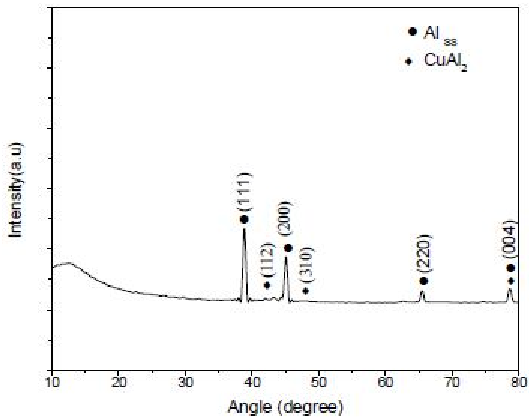

Fig.10. The XRD pattern of artificially aged 2014 aluminum alloy at 183 ˚C, 6 hrs.

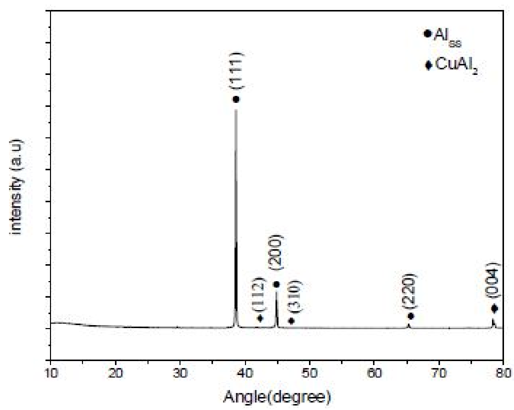

Fig.11. The XRD pattern of artificially aged 2014 aluminum alloy at 183 ˚C, 8 hrs.

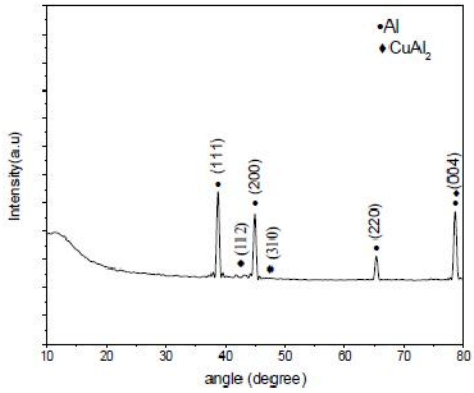

Fig.12. The XRD pattern of artificially aged 2014 aluminum alloy at 183 ˚C, 10 hrs.

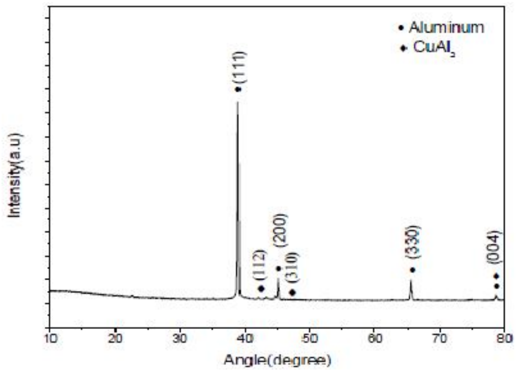

Fig.13. The XRD pattern of artificially aged 2014 aluminum alloy at 183 ˚C, 12 hrs.

3.3 HARDNESS MEASUREMENTS

The hardness value after solution treatment is measured 94 BHN

T able 2: Brinell hardness value of AA2014 Alloy after Aging.

S. No.	Time (hours)	Hardness (BHN)
1	2	103
2	4	106
3	6	117
4	8	129
5	10	107
6	12	101

3.4 AGING CURVE OF AA2014 ALLOY

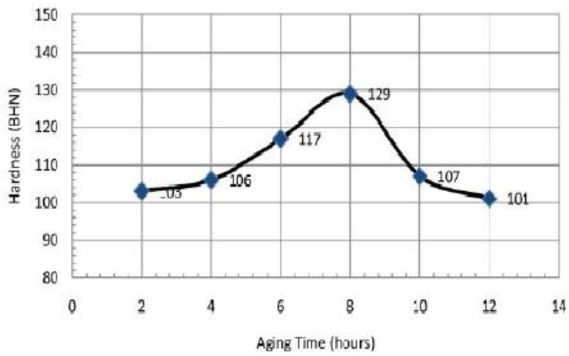

Fig.14. Aging curve of AA2014 aluminum alloy artificially aged at 183 ° C.

Fig. 2 shows the microstructure of alloy artificially aged at 183 ⁰C for 4 hours. The microstructure reveals some more $CuAl_2$ precipitates (dark) has formed in the aluminum matrix (bright). The precipitation sequence is reported as follows: SSSS (α-Al)→ GP zones → α+θ'' → α+θ' → α+θ. Fig. 3 shows the microstructure of 2014 aluminum alloy artificially aged for 6 hours. The microstructure reveals some more amount of $CuAl_2$ precipitates (dark) compared to the specimen aged for 2 and 4 hours in the aluminum matrix (bright). This will lead to some more increase in hardness. Fig. 4 represents the microstructure of alloy artificially aged at 183 ⁰C for 8 hours. This microstructure reveals the maximum amount of $CuAl_2$ precipitates and AlCuMgSi (dark) in the aluminum matrix (bright). The largest value of hardness is measured on this specimen. Fig. 5 shows the microstructure of 2014 aluminum alloy aged for 12 hours. This microstructure reveals more coarsened $CuAl_2$ precipitate particles (dark) in the aluminum matrix (bright). The drop in hardness is found in this specimen. This drop in hardness is due to loss of coherency between $CuAl_2$ precipitate particles and matrix.

Fig.6 shows the XRD pattern of as received AA2014 aluminum alloy. We observed four major peaks in the pattern. These peaks are found at 39.13°, 45.53°, 65.83° and 78.8° angles respectively. The minor peaks are found at 42.5°, 47.5° and 83.1° angles respectively. The major peaks are identified as aluminum solid solution while the minor peaks are of $CuAl_2$. The highest intensity peak is found at 39.13° on (111) plane. Fig. 7 shows the XRD pattern of solution treated 2014 aluminum alloy. In this pattern only four major peaks are observed. And these peaks are found at 38.82°, 45.14°, 65.5°and 78.5° angles respectively. After analysis these peaks are identified as aluminum solid solution. Due to entire dissolution of $CuAl_2$ precipitates in aluminum matrix the peaks of $CuAl_2$ are absent. The highest intensity peak is found at 38.82° on the (111) plane. The highest peak in the solution treated sample is found at lower angle than as received sample due dissolution of precipitate resulting removal of the strains. Fig.8-9 show the XRD pattern of artificially aged 2014 aluminum alloy at 183℃ for 2 & 4 hrs. Four major peaks are observed in the pattern. The peaks are found at 38.78°, 45.06°, 65.44° and 78.55° respectively. Fig.10 shows that out of four peaks, three peaks are identified as aluminum solid solution and peak found at 78.55° is the peak of $CuAl_2$ precipitate as well as of aluminum solid solution .The highest intensity peak is found at 38.78° on (111) plane. Fig. 11 shows the XRD pattern of artificially aged 2014 aluminum alloy at 183℃ for 8 hrs. The four major peaks are found in the pattern. The peaks are at 38.59°, 44.91°, 65.30°and 78.48° respectively. The minor peaks are of $CuAl_2$ found at 42.5° and 47.5° angles respectively. These peaks are identified as aluminum solid solution and $CuAl_2$ precipitate. Highest intensity is peak found at 38.59° on (111) plane. Fig.12-13 shows the XRD pattern of artificially aged alloy at 183 °C, for 10 hrs and 12 hrs. The four major peaks are found in the pattern. These are at 38.64°, 44.93°, 65.30° and 78.42° respectively. These peaks are identified as aluminum solid solution and $CuAl_2$ precipitate .Highest intensity peak is found at 38.64°on (111) plane. The Fig. 10 represents increased intensity of $CuAl_2$ due to coarsened precipitate particles.

It clear from the microstructures (Fig. 2-5) that the precipitate particles are responsible for the strain in the matrix. The age hardening curve represents (Fig. 14) the variations of hardness due to the formation of the $CuAl_2$ precipitates. As the number of $CuAl_2$ precipitate particles increases the value of hardness also increases. After aging time of 2 hours the hardness is found BHN 103. The hardness increases with increasing aging time. The maximum hardness is measured BHN 129 for the aging time of 8 hours. For the aging time more than the 8 hours, the hardness values are decreasing due to the coarsening of the $CuAl_2$ precipitate particles leading to loss in coherency between the $CuAl_2$ precipitate particles and the aluminum matrix which results decrease in strength. When the precipitate particles are coherent with the matrix then they participate as a member of continuous matrix under the loading conditions but as the size of precipitate particle increases, it starts loosing coherency and finally it becomes a separate particle inside the matrix. Now, these precipitates are no more part of continuous matrix and they do not share loads under the loading conditions. By the XRD analysis, we found the major peaks at 39.13°, 45.53°, 65.83°, 78.8° and 83.17° respectively in as received specimen while in solution heat treated sample, the peaks are found at 38.82°, 45.14°, 65.5°and 78.5° respectively. This shows that after solution treatment the peaks shift to the lower angles. In artificially aged 2014 aluminum alloy at 183 °C for 2 hours, even though the $CuAl_2$ precipitate particles are formed but their peaks are not detected. Because of their phase fraction is less than 4 – 5%. As aging time increases $CuAl_2$ peaks are detected along with aluminum solid solution peaks. In the 2014 aluminum alloy specimen aged for 8 hours , peaks are found at 38.59°, 42.5°, 44.91°, 47.5°, 65.30°and 78.48° respectively. Here, the peak of $CuAl_2$ is detected at 42.5°, 47.5° and 78.48°on the (112), (310) and (004) planes respectively.

CONCLUSIONS

The microstructures clearly revealed $CuAl_2$ precipitate particles in the aluminum matrix. The measured hardness value of as received AA2014 alloy is 121 BHN. The solution heat treated AA2014 aluminum alloy has hardness value of 94 BHN which is decreased compared to as received sample due to single phase solid solution. As aging time increases, the hardness values keep on increasing upto 8 hrs of aging and thereafter these values are found decreased for aging of 10 hrs and 12 hrs. Highest hardness value 129 BHN is obtained after the aging of 8 hours. The peaks which are observed in the XRD pattern of artificially aged AA2014 aluminum alloy are shifted to lower angles compared to as received sample. In artificially aged 2014 aluminum alloy for 8 hours, peaks are found at 38.59˚, 42.5˚, 44.91˚, 47.5˚ 65.30˚and 78.48˚ angles respectively. The peaks of $CuAl_2$ are detected at 42.5˚, 47.5˚ and 78.48˚on the (112), (310) and (004) planes respectively.

REFERENCES

[1] Jae-Ho JANG, "Effect of solution treatment and artificial aging on Microstructure and mechanical properties of al-cu alloy", Bussan 618- 230, pp 631, 2012.

[2] Juraj Belan, "Metallography of alloys used in aircraft jet engine construction", University of Žilina, pp 148 - 152.

[3] E.A. Starke, J.P. Staley, "Prog. Aerosp.", Sci. 32, 131-172, 1996.

[4] M. Gavgali, B. Aksakal, Mater. Sci. &Engg., A 254, 189, 1998.

[5] "A Statistical Review on Aluminium Shipment by Major Market: United States and Canada", Alcoa Technical Centre, Alcoa Centre, PA, USA, 2006.

[6] I. Sabirov, M.Yu Murashkin, R.Z. Valiev, Mater. Sci. Eng., 560, 1-24, 2013.

[7] S.K. Panigrahi, R. Jayaganthan, Metall. Mater. Trans., A 41, 2675-2690, 2010.

[8] D. Singh, P.N. Rao, R. Jayaganthan, Mater. &Des 50, 646-655, 2 013.

[9] T. Shanmugasundaram, B.S. Murty, V.S.S. Sarma, Scr. Mater 54, 2013-2017, 2006.

[10] S.K. Panigrahi, R. Jayaganthan, Mater. Des. 32, 3150-3160, 2011.

[11] R.Z. Valiev, R.K. Islamgaliev, I.V. Alexandrov, Prog. Mater. Sci. 45, 103-189, 2000.

[12] R.Z. Valiev, Y. Estrin, Z. Horita, T.G. Langdon, M.J. Zehetbauer, Y.T. Zhu, Nanostr. Mater, 33-39, 2006.

[13] Y.B. Lee, D.H. Shin, K.T. Park, W.J. Nam, Scr. Metal. 51, 355-359, 2004.

[14] V.S. Sarma, K. Sivaprasad, D. Sturm, M. Heilmaier, Mat. Sci. Eng. A 489, 253-258, 2008.

[15] S.K. Panigrahi, R. Jayaganthan, J. Mat. Sci. 45, 5624-5636, 2010.

[16] S.K. Panigrahi, R. Jayaganthan, Metall. Mater. Trans. A 42, 3208-3217, 2011.

[17] P. Bassani, E. Gariboldi, G. Vimercati, J. Therm. Anal. Comp. 87, 247-253, 2007.

[18] S.K. Varma, D. Salas, E. Corral, E. Esquivel, J. Mat. Sci. 34, 1855-1863, 1999.

[19] M.A. Nikitina, R.K. Islamgaliev, A.F. Kamalov, Mater. Sci. Forum 667, 331-336, 2011.

[20] J. Mao, S.B. Kang, J.O. Park, J. Mat. Proc. Tech. 159, 314-320, 2005.

[21] T. Shanmugasundaram, M. Heilmaier, V.S. Sarma, B.S. Murty, Mater. Sci. Forum 690, 234-237, 2011.

[22] J. Wang, Y. Iwahashi, Z. Horita, M. Furukawa, M. Nemoto, R.Z. Valiev,T.G. Langdon, Acta Metall. 44, 2973-2982, 1996.

[23] K.T. Park, H.J. Kwon, W.J. Kim, Y.S. Kim, Mater. Sci. Eng. A 316, 145-152, 2001.

[24] F. Zhou, J. Lee, S. Dallek, E.J. Lavernia, J. Mater. Res. 16, 3451-3458, 2001.

★★★